AIDIC *Conference Series*, Vol. 10, 2011
Editor Sauro Pierucci
DOI: 10.3303/ACOS1110018

ISBN 978-88-95608-58-7 ISSN 2036-5969

METAL DISPLACEMENT DEPOSITION: A NEW ROUTE FOR TEMPLATE FABRICATION OF METAL AND METAL OXIDE NANOSTRUCTURES

Rosalinda Inguanta*, Germano Ferrara, Salvatore Piazza, Carmelo Sunseri

Laboratorio di Chimica Fisica Applicata, Dipartimento di Ingegneria Chimica, Gestionale, Informatica e Meccanica, Università di Palermo
Viale delle Scienze, 90128 Palermo (Italy), *rosalinda.ingunta@unipa.it

We have grown ordered arrays of metal and metal oxide nanostructures inside pores of anodic alumina templates using displacement reactions. This method is based on the galvanic contact between a sputtered metal film, covering the bottom of the template, and a less noble metal, partially exposed to the solution. In the case of metal nanostructure synthesis, dissolution of the sacrificial anode is accompanied by reduction of metal ions into template pores; here we report examples concerning Cu and Pd nanowires fabrication. For metal oxide nanostructures, nitrate solutions were employed: anodic dissolution then provokes reduction of nitrate ions and base-generation. The latter increases greatly pH into template channels inducing oxide precipitation; the current-less fabrication of LnO/OH (Ln = La, Ce, Sm, Er) nanostructures will be described.

1. INTRODUCTION

Nanostructured materials, having at least one dimension of the order of nanometers, present often properties different from those of bulk materials (Kelsall et al., 2005), which make them highly attractive for several technological applications. Among nanostructured materials, one-dimensional ones, like nanowires (NWs) and nanotubes (NTs), are of particular interest. Among techniques used to fabricate this kind of materials, template synthesis within nanoporous membranes is particularly simple and flexible (Martin, 1996). In fact, this technique allows producing ordered arrays of one-dimensional nanostructures with different aspect ratios and different shapes (Inguanta et al., 2009a). In this context, anodic alumina membrane (AAM) is considered an almost ideal "template" for the synthesis of nanostructured materials, to be used in various applications such as optoelectronics, magnetic sensors and electronic circuits (Shingubara, 2003). In addition, the interest in anodic alumina membranes is also due to the simplicity of their fabrication process. In fact, they can be obtained by anodizing aluminum in appropriate acidic baths, and this leads to the formation of nanoporous honeycomb structures, whose morphological parameters (membrane thickness, pore diameter and density) can be easily controlled by adjusting experimental parameters (anodizing voltage and time, bath temperature and composition) (Inguanta et al., 2007a). For these reasons, various nanostructures (metals, alloys, semiconductors, oxides and polymers) with different morphologies (tubules, fibers or wires) have been fabricated using AAM as template. The most common techniques used for template synthesis are the sol-gel process (Zhang et Chen, 2005), the microwave plasma chemical vapor deposition (Chen et al., 2007), the electrodeposition and the electroless deposition (Inguanta et al., 2007a, 2007b, 2010). A drawback common to these techniques is that their implementation requires use of expensive reagents and equipment: for example, electrodeposition is flexible and allows a control on the nanostructure, acting on the electrical parameters (Inguanta et al., 2011; Ferrara et al., 2010, 2011), but it needs an external power source. By contrast, electroless deposition does not require electrical energy, but it presents particular drawbacks: cost of reagents (chelating agent, bath stabilizers, buffers for pH control), long deposition times (steps for cleaning and activation of the substrate), control of the kinetic of reaction. Besides, in the case of deposition inside membrane pores, it is essential to avoid that reduction occurs in the bulk of the solution, which should lead to the formation of a thick deposit layer onto the external surface

Please cite this article as: Inguanta R., Ferrara G., Piazza S. and Sunseri C., (2011), Metal displacement deposition: a new route for template fabrication of metal and metal oxide nanostructures, AIDIC Conference Series, 10, 159-168
DOI: 10.3303/ACOS1110018

of the membrane, blocking pore mouth and thus preventing nanostructure formation. In addition, metal deposits obtained by electroless deposition display in many cases low purity, because they contain impurities deriving from the deposition bath. In this work, we present the current-less fabrication of nanostructures of metal (Inguanta et al., 2008, 2009b) and metal oxide, by a novel technique, based on the cementation reaction of metal ions in solution (Inguanta et al., 2007c) using a sacrificial anode as a reducing agent. Using a special arrangement, a galvanic couple is formed between a low noble metal (Al or Zn), partially exposed to the electrolytic solution, and a thin gold layer, covering pore bottom of the membrane. In this way, dissolution of the sacrificial anode is coupled to a cathodic reduction, which is forced to occur within template channels; final result of the cementation process is the growth of nearly one-dimensional nanostuctures having the desired composition. Purpose of this study is to verify the potential of this technique for the fabrication of nanostructured metals and oxides with high purity, using an appropriate precursor salt solution.

2. EXPERIMENTAL DETAILS

Aluminium (thickness: 1.5 mm, purity: 99.99%) or zinc (thickness: 2 mm, purity: 99.99%) foil has been used as sacrificial anode for the cementation process, owing to their very nobility. Commercial anodic alumina membranes (AAM, Whatman, Anodisc 47) were used as template, having a mean pore diameter of about 210 nm, nominal thickness of 60 μm, porosity of about 28% and pore surface density of 10^{13} pores/m^2. Before deposition, one membrane external surface was covered with gold, coupled electrically to the less noble metal through a conductive paste and delimited by a insulating lacquer. After immersion of the bimetallic couple into the electrolytic solution, containing a metal ion, a micro-battery is formed, where gold acts as cathode and the less noble metal as anode (see Fig.1); in the first case (Fig.1a) anodic dissolution of the sacrificial anode is coupled to reduction of metallic ions within template pores, leading to formation of a metal nanostructure; in the second case (Fig.1b) the anodic dissolution process is accompanied by nitrate ions reduction, with generation of hydroxyl ions into membrane channel: the steep rise of local pH provokes precipitation of a lanthanide oxy/hydroxide in form of nanostructure.

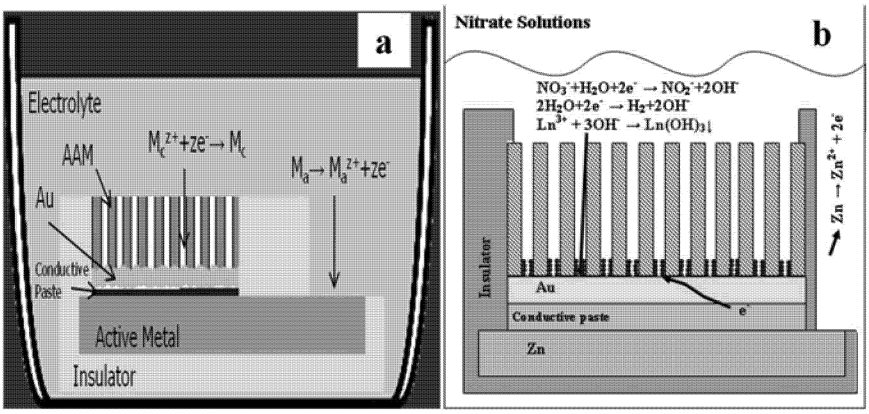

Fig. 1: Schematic representation of the galvanic cell designed for the fabrication of nanostructured metals (a) and oxides (b) inside the channels of an alumina template.

Cementation solutions were prepared using deionised water and high purity chemical reagents. Table 1 reports the composition of cementation solutions used for the fabrication of metal and metal oxide nanostructures. Depositions were carried out at different temperatures and for different cementation times. Morphological and structural characterization of the nanostructure was carried by Scanning Electron Microscopy (SEM), Energy Dispersive Spectroscopy (EDS), X-ray diffraction (XRD) and RAMAN spectroscopy. Details on the investigation techniques adopted can be found elsewhere (Inguanta et al., 2007b, 2010).

Table 1: Cementation solution

Deposit	Solution	Concentration	pH
Cu	$CuSO_4 + H_3BO_3$	0.2 M + 0.1 M	3
Pd	$Pd(NH_3)_4(NO_3)_2 + H_3BO_3$	7 mM + 0.1 M	6.6
$Ln(OH)_3/Ln_xO_y$	$Ln(NO_3)_3$ (Ln = La, Ce, Sm, Er)	0.1 M	2.6÷5.2

3. RESULTS AND DISCUSSION

The galvanic deposition process allows obtain high-purity nanostructures in a simple and inexpensive way. This procedure is based on a cementation reaction that produces the desired nanostructure inside the AAM template pores. The peculiarity of this method is that the electromotive force for the deposition process must not be supplied from an external source. Another advantage is the possibility to vary the ratio between anode and cathode surface area in order to control the deposition rate. Moreover, we will show that this method is very flexible because it can be used for deposition of both metal and metal oxide nanostructures with different shapes (NWs and NTs). In the following we will describe briefly results pertaining to the formation of metallic NWs (Cu, Pd), using the arrangement shown in Fig.1a, and to the fabrication of nanostructured lanthanides oxy/hydroxides (in form of NWs and/or NTs), using the arrangement shown in Fig.1b. Details on the results regarding the single nanostructure can be found in the literature quoted.

3.1 Cementation of metal nanostructures

In the case of copper cementation, we used Al as sacrificial anode and a acidic deposition solution containing copper sulphate salt (Inguanta et al., 2008). Ratio between membrane and anodic area was set to 4 and deposition was performed at room temperature. In such conditions, the standard potential for Cu^{2+} reduction to Cu^0 is much higher than that of the Al^{3+}/Al^0 redox couple; thus the displacement reaction occurs, according to Fig.1a:

$$3Cu^{2+} + 2Al = 3Cu + 2Al^{3+} \quad (1)$$

Consequence of reaction (1) was the growth of copper nanowires whose height increased with increasing cementation time.

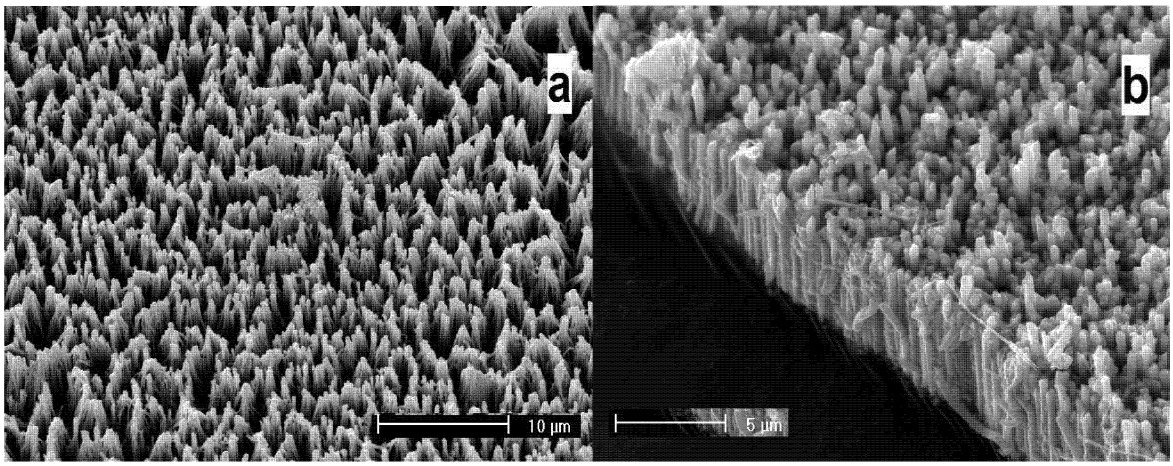

Fig. 2: SEM images, taken after dissolution of the AAM template, of copper (a) and of palladium (b) nanowires obtained by displacement deposition reaction.

After 7 h of cementation NWs were about 2.5 μm long, whilst after 3 days their length reached a value of about 44 μm, quite uniform in all pores; after one week reaction (1) led to a complete pore filling and to the growth of an external metal layer of about 100 μm.
In all deposition conditions, morphology of Cu NWs was similar the FEG-SEM image of Fig. 2(a). NWs are straight with a cylindrical shape; their uniform diameter (about 210 nm) is almost equal to the size of the AAM channels. Template dissolution does not alter the alignment between NWs, which are firmly hammered in the thin gold layer. The presence of some broken NWs is due to sample preparation before FEG-SEM analysis. Since the Cu deposition occurred in all pores, NWs surface density was equal to pore population of the AAM (of the order of 10^{13} wires m^{-2}).
EDS spectra showed that NWs consist of pure copper metal. This finding was confirmed by X-ray diffractograms, revealing a polycrystalline structure of the deposited metal. Identification of peaks, which are relative to the cubic structure of copper, was performed by comparison with the ICDD data-base (card n. 4–836).
Similar results were obtained in the case of fabrication of palladium NWs by displacement of Al or Zn in a quasi-neutral electrolyte containing a Pd nitrate salt (Inguanta et al, 2009b). In this case the cathodic deposition reaction is:

$$Pd(NH_3)_4^{2+} + 4H_2O + 2e^- = Pd + 4NH_4^+ + OH^- \quad (2)$$

Standard potential of this reaction (0. 0 V vs. NHE) is far positive with respect to the equilibrium potential of the Al^{3+}/Al^0 couple; moreover nitrate ions reduction occurs in solution, leading to further hydroxyl ions generation.
Also in this case, NWs filled uniformly all template channels and they consisted of pure and polycrystalline (ICDD card n. 46–1043) palladium metal, with XRD peaks belonging to the face-centered cubic phase of Pd, and an average grain size of about 3 nm. Figure 2(b) shows an array of Pd NWs obtained by this way: NWs are straight with a cylindrical shape. The diameter is uniform and almost equal to the size of the AAM channels and the contour is very smooth. NWs height was uniform and it varied with the cementation time from about 1.5 μm to 9 μm, in dependence also of the anodic to cathodic area ratio; the latter was changed 0.25 to 1 in different experiments. However, a reduction in NWs growth rate was observed for long cementation times, likely due to a progressive deactivation of the cathodic surface.
Similar results were obtained short after by Xu and co-workers (Xu et al, 2009) using the same approach. Their results show that it was possible to grow by galvanic displacement also nanowires of other metals, like Au, Ni, Pt and Co.

3.2 Cementation of metal oxide/hydroxide nanostructures

Recently, we have extended successfully the displacement deposition technique to the fabrication of large arrays of self-standing oxide nanostructures. In order to obtain a metal oxy/hydroxide, the metal salt contained in the electrolytic bath plays a key role. In fact, when a metal nitrate solution was used, reduction of the NO_3^- anion is able to guide the deposition reaction towards formation of oxide phases instead of metal ones (Mondal et al., 2006). In particular, precipitation of oxy/hydroxide happens when the standard potential for NO_3^- reduction is higher than that of the corresponding metal phase. Using the arrangement shown in fig.1b, sacrificial metal dissolution occurs, accompanied by the following reactions at cathode surface:

$$NO_3^- + H_2O + 2e^- = NO_2^- + 2OH^- \quad (3)$$

$$Me^{z+} + zOH^- = MeOH_x \rightarrow MeO_x \quad (4)$$

Reaction (4) leads to precipitation of a nanostructured oxy/hydroxide within the channels of the alumina template. Relatively short deposition times are necessary to grow large and ordered arrays of oxide nanostructures. We have investigated the cementation process in nitrate solutions of Co, Ni, Zn, Pb and Ln (Ln=

La, Ce, Sm, Er). In the following we will report examples regarding the fabrication of nanostructures of rare earth metal oxy/hydroxides (LnO/OH) using Zn as sacrificial electrode, and anodic and cathodic areas exposed to the solution both equal to 1 cm^2. After immersion in the electrolyte containing Ln^{3+} ions, we observed a progressive and uniform filling of all AAM channels owing to the formation of lanthanide oxy/hydroxide nanostructures. Table 1 reports the height of nanostructures after different cementation times at room temperature: it is evident that growth is faster up to 24 hours, after which nanostructures height changes slightly.

Table 2: Ln oxide nanostructures height after different cementation times at 25 °C.

Sample	Time	La	Ce	Sm	Er
Ln12	3h	6.5	18.09	7.25	23.9
Ln2	24h	40.03	42.63	41.33	42.27
Ln1	72h	46.06	48.37	46.13	47.82
Ln8	168h	50.42	53.7	48.77	52.4
Morphology		NTs+NWs	NTs	NWs+NTs	NTs

This reduced growth rate can be ascribed mainly to a progressive deactivation of the anode surface, caused by its partial passivation (Inguanta et al., *Submitted*): in fact a faster hydroxyl generation with respect to its consumption by reaction (4), causes an increase of solution bulk pH (see Fig.3) during the first hours of immersion, with consequent precipitation of oxides also onto the anodic surface.

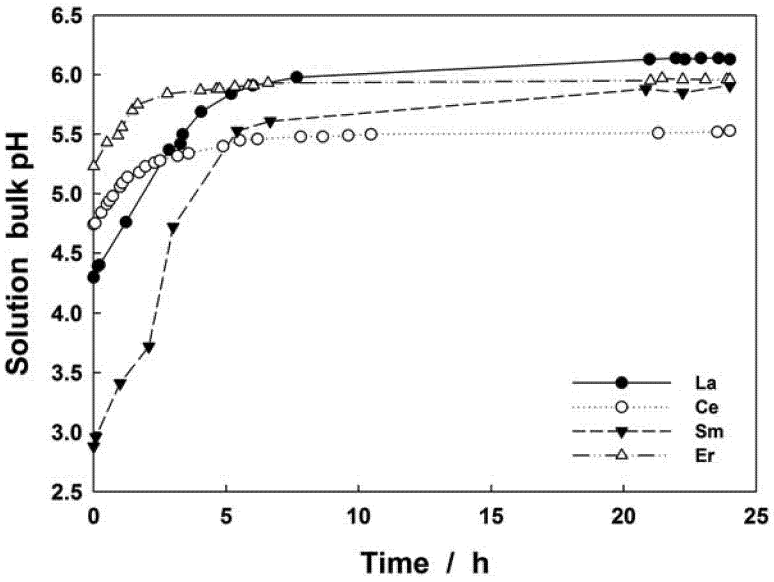

Fig. 3: Bulk solution pH during formation of LnO/OH nanostructures at room temperature.

A contribution to electrolyte pH increase comes out also from the side reaction of hydrogen evolution, occurring also at gold surface, whose presence is revealed by evolution of hydrogen bubbles form the surface of alumina template during the cementation process.

In these experimental conditions, a complete filling of alumina pores was obtained after one week of cementation at room temperature: after this time a thin and compact layer of lanthanide oxy/hydroxide was formed on the external surface of the template exposed to the solution. However, nanostructure morphology was different depending on the lanthanide species (Inguanta et al., *Submitted*). Fig.4 displays SEM images (obtained

after template dissolution by alkaline etching) of samples after 24 hours deposition at room temperature: only tubular shape is observed for Er and Ce nanostructures, having almost equal heights (about 45 μm), whilst both oxide NWs and NTs are grown during cementation of La and Sm.

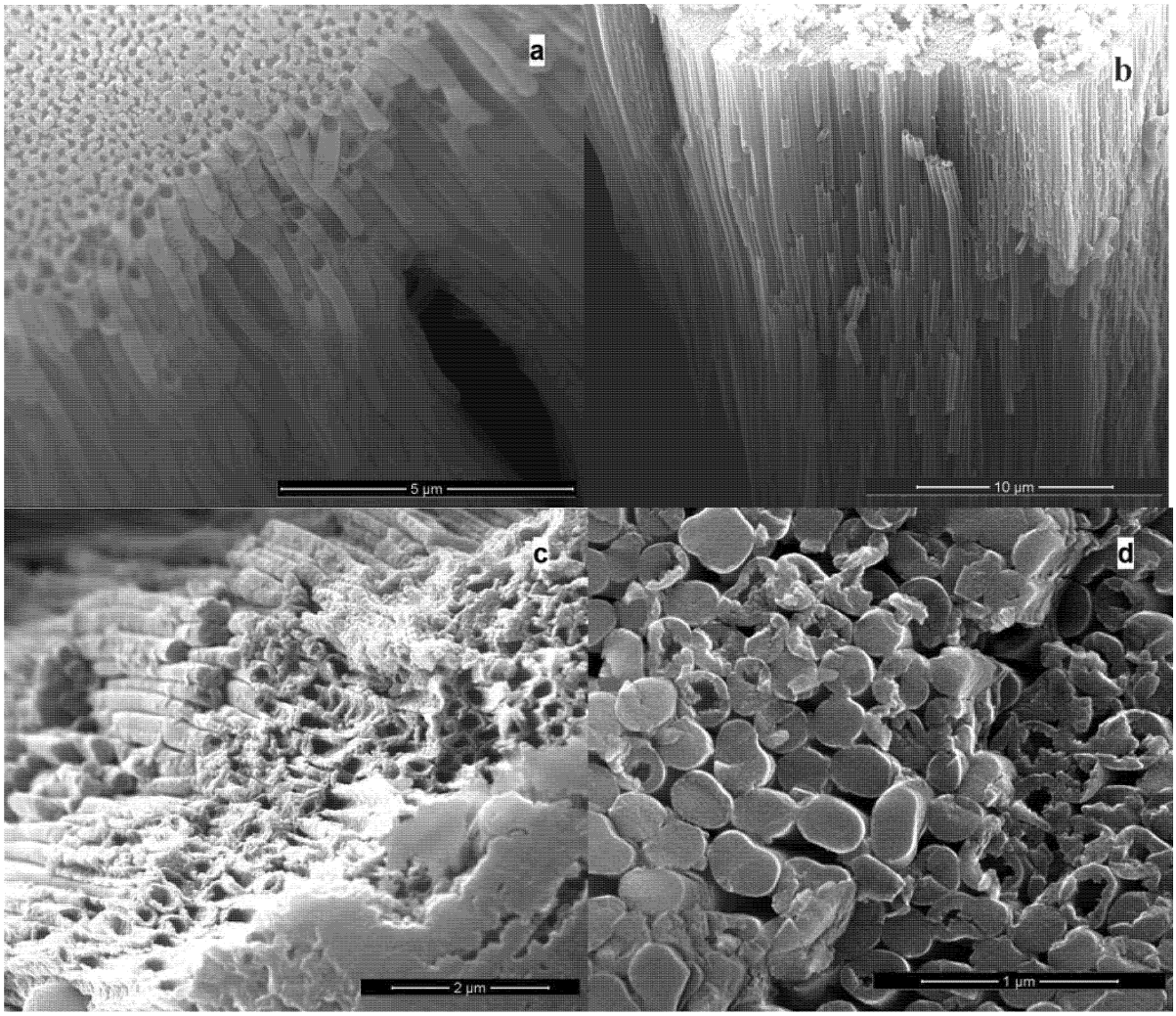

Fig. 4: SEM images of LnO/OH nanostructures obtained after 24 h displacement deposition at room temperature. : (a) Er oxy/hydroxide; (b) Ce oxy/hydroxide; (c) La oxy/hydroxide; (d) Sm oxy/hydroxide.

It is worth to note that nanostructure morphology is strongly influenced by deposition temperature (Inguanta et al., Submitted): performing cementation at 6°C only NTs, having uniform wall thickness along their height, were obtained for all lanthanides, whilst at 60°C only NWs were formed; moreover, in the last case nanostructures are sensibly shorter than those obtained at lower temperature for corresponding cementation times, and they seem to present a limiting height. This complex behaviour can be related to the growth mechanism of nanostructures and to the different transport rate of Ln^{3+} ions from pore mouth to the reacting site.
As for oxides structure and composition, we have performed EDS, XRD and Raman analyses for each experiment after different cementation times (i.e., at different heights). Purity of the LnO/OH nanostructures is confirmed by EDS analysis, showing the presence of only Ln and O in almost all experiments; an EDS spectrum is reported in Fig.5a taken after 24 h of deposition of cerium oxide at room temperature: peaks of C, Al and Au are due to the SEM specimen holder, to the residual alumina template, and to the gold film sputtered onto the

surface sample before SEM analysis, respectively. Only for very long cementation times (more than 72 h) the appearance of Zn peaks reveals contamination of the nanostructure due to some co-precipitation of ZnO. Regardless of deposition temperature, LnO/OH nanostructures present a disordered or nanocrystalline structure. Indeed X-ray diffraction patterns show no reliable peaks in almost all cases, with the exception of ceria nanostructures, for which deposit was characterized by the presence of broad reflections with low intensity (Fig.5b), assigned to CeO_2 phase. Using the Shrerrer's formula (West, 1985), from the main peak area we estimated grain size of ceria nanostructures varying between 3 and 8 nm, slightly increasing with cementation temperature.

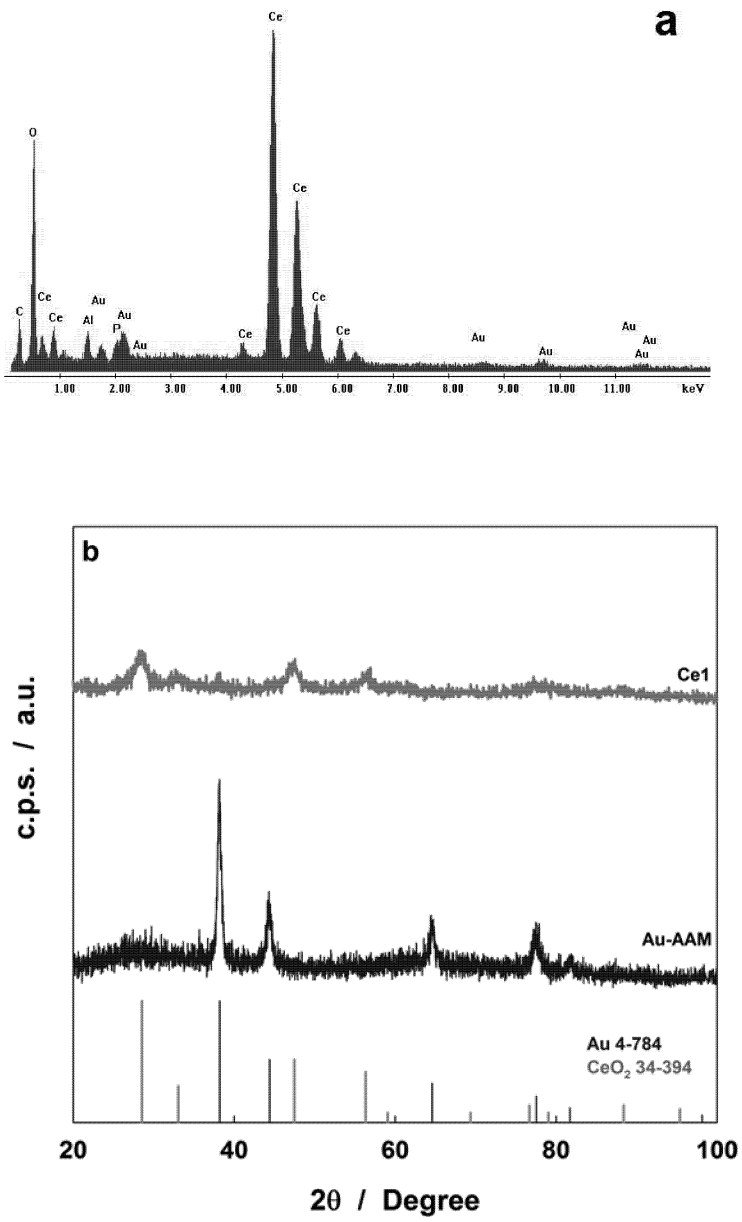

Fig. 5: (a) EDS spectrum of CeO/OH nanostructure obtained after 24 h displacement deposition at room temperature. (b) XRD diffraction patterns of CeO_2 nanotubes.

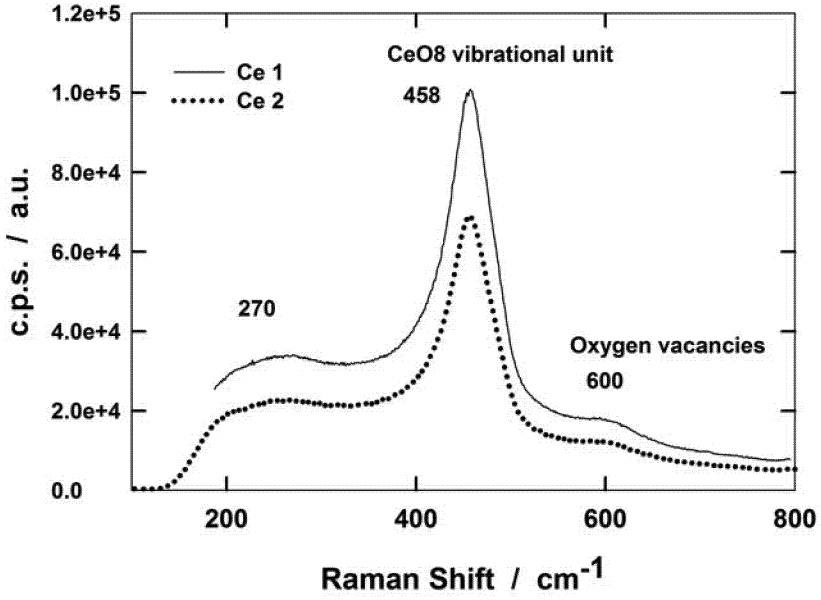

Fig. 6: Raman spectra of CeO_2 nanostructures obtained after different cementation times at room temperature.

Grain size of ceria nanostructures was confirmed by Raman spectra, shown in Fig.6: the main peak at wavenumber of about 458 cm^{-1} can be assigned to a symmetrically stretching of the Ce-O8 vibrational unit in the ceria phase (Kosacki et al., 2002). From the half-peak width of this mode it is possible to calculate the grain size of ceria nanostructures, in good agreement with those of XRD analysis. It is important to highlight that shift and asymmetry of the main Raman line are both due to the nanometer dimension of grain size, as well as to the presence of oxygen vacancies, as reported in (Inguanta et al., 2007b; Halaoui et al., 2009); the presence of oxygen vacancies is further confirmed by the Raman mode at 600 cm^{-1}. Moreover, the absence of peaks located at 740 and 1049 cm^{-1} indicates that ceria deposit is not contaminated by nitrate ions present in the cementation bath. For the other lanthanide oxy/hydroxides, the absence of any characteristic Raman mode in the spectra confirms the hypothesis that in those cases cementation produces amorphous nanostructures, in agreement with the results of the XRD investigation.

4. CONCLUSIONS

We have used displacement deposition reactions to fabricate metal and metal oxide nanostructures. For this aim, a galvanic couple was formed between a metal sacrificial anode (Al or Zn) and the Au thin layer that covering pore bottom of the template, originating a cementation reaction at pore bottom. It has been demonstrated that employing this technique it is possible to synthesize nanostructures of metals or oxides with different shapes (nanowires and/or nanotubes) and aspect ratios (height/width). Examples are reported concerning the fabrication of Cu and Pd metallic nanowires, and nanostructured lanthanide oxides, in form of nanotubes and/or nanowires. In all cases the nanostructures synthesized present high purity.

The key advantages of this fabrication technique are its simplicity and low cost, because it does not need any external power source and makes use of aqueous electrolytes. Moreover, the technique is versatile, because it allows deposition of different materials (metals, oxides, but also semiconductors) and morphological shapes, and easy to extend to much larger deposition area.

5. REFERENCES

Chen M., Pan M., Hung I., Wu C. and Chen F., 2007, Amorphous carbon coated silicon nano-tips fabricated by microwave plasma chemical vapor deposition using anodic aluminium oxide as the template, J Electrochem. Soc., 154; D215-D219

Ferrara G., Inguanta R., Piazza S. and Sunseri C., 2010, Electrosynthesis of Sn-Co nanowires in alumina membranes, J Nanosci. Nanotech. 10, 8328-8335.

Ferrara G., Damen L.; Arbizzani C., Inguanta R., Piazza S., Sunseri C., and Mastragostino M., 2011, Sn-Co nanowires array as negative electrode for lithium-ion batteries, J Power Sources, 196, 1496-1473.

Hamlaoui Y., Pedraza F., Remazeilles C., Cohendoz S., Rebere C., Tifouti L., Creus J., 2009, Cathodic electrodeposition of cerium-based oxides on carbon steel from concentrated cerium nitrate solutions Part I. Electrochemical and analytical characterization, Mater. Chem. Phys., 113, 650-657.

Inguanta R., Butera M., Sunseri C. and Piazza S., 2007a, Fabrication of metal nano-structures using anodic alumina membranes grown in phosphoric acid solution: Tailoring template morphology, Appl. Surf. Sci. 253, 5447-5456

Inguanta R., Piazza S. and Sunseri C., 2007b, Template electrosynthesis of CeO_2 nanotubes, Nanotechnology, 18, 561-566.

Inguanta R., Piazza S. and Sunseri C., 2007c, Metodo e apparato per la fabbricazione di nanowires metallici, Patent, I.P. VI2007A000275.

Inguanta R., Piazza S. and Sunseri C., 2008, Novel procedure for the template synthesis of metal nanostructures, Electrochem. Comm., 10, 506-509.

Inguanta R., Ferrara G., Piazza S. and Sunseri C., 2009a, Nanostructures fabrication by template deposition into anodic alumina membranes, Chem. Eng. Trans. 17, 957-962.

Inguanta R., Piazza S., and Sunseri C., 2009b, Synthesis of self-standing Pd nanowires via galvanic displacement deposition, Electrochem. Comm., 11, 1385-1388.

Inguanta R., Livreri P., Piazza S. and Sunseri C., 2010, Fabrication and photoelectrochemical behavior of ordered CIGS nanowire arrays for application in solar cells, Electrochem. Solid State Lett., 13, K22-K25.

Inguanta R., Vergottini F., Ferrara G.; Piazza S. and Sunseri C., 2011, Effect of temperature on the growth of □-PbO2 nanostructures, Electrochem. Acta, 55, 8556-8562.

Inguanta, R.; Ferrara, G.; Piazza, S.; Sunseri, C. A new route to grow oxide nanostructures based on metal displacement deposition. I Lanthanides oxy/hydroxides growth. Submitted

Inguanta, R.; Ferrara, G.; Piazza, S.; Sunseri, C. A new route to grow oxide nanostructures based on metal displacement deposition. II Lanthanides oxy/hydroxides characterization. Submitted

Kelsall R. and Hamley I., 2005, Nanoscale Science & Technology. Wiley, Chichester.

Kosacki I., Suzuki T., Anderson H. U., Colomban, P., 2002, Raman scattering and lattice defects in nanocrystalline CeO_2 thin films, Solid State Ionics, 149, 99-105.

Martin C. R., 1996, Membrane-Based Synthesis of Nanomaterials, Chem. Mater., 8, 1739-1746.

Mondal A., Mukherjee N., Bhar S.K., 2006, Galvanic deposition of hexagonal ZnO thin films on TCO glass substrate, Mater. Lett., 60, 1748-1752.

Pauvonic M. and Schlesinger M., 2000, Modern Electroplating, Wiley, New York.

Shingubara S., 2003, Fabrication of nanomaterials using porous alumina template, J. Nanopart. Res. 5, 17-30

West A.R, 1985, Solid State Chemistry and its Applications, John Wiley & Sons Ltd, Chichester

Zhang G. and Chen J., 2005, Synthesis and Application of $La0.59Ca0.41CoO_3$ Nanotubes, J Electrochem. Soc. 152, A2069-A2073

Xu Q., Meng G., Wu X., Wei Q., Kong M., Zhu X., Chu Z., 2009, A generic approach to desired metallic nanowires inside native porous alumina template via redox reaction, Chem. Mater., 21, 2397-2402.